ELSEVIER

Journal of Power Sources 112 (2002) 634–638

JOURNAL OF POWER SOURCES

www.elsevier.com/locate/jpowsour

Short communication

Synthesis and electrochemical properties of $Li[Li_{(1-2x)/3}Ni_xMn_{(2-x)/3}]O_2$ as cathode materials for lithium secondary batteries

S.-S. Shin[a], Y.-K. Sun[a,*], K. Amine[b]

[a]*Department of Chemical Engineering, Hanyang University Seungdong-Gu, Seoul 133-791, South Korea*
[b]*Electrochemical Technology Program, Chemical Technology Division, Argonne National Laboratory, Argonne, IL 60439, USA*

Received 20 May 2002; accepted 5 August 2002

Abstract

Layered $Li[Li_{(1-2x)/3}Ni_xMn_{(2-x)/3}]O_2$ materials with $x = 0.41$, 0.35, 0.275 and 0.2 are synthesized by means of a sol–gel method. The layered structure is stabilized by a solid solution between $LiNiO_2$ and Li_2MnO_3. The discharge capacity increases with increasing lithium content at the 3a sites in the $Li[Li_{(1-2x)/3}Ni_xMn_{(2-x)/3}]O_2$. A $Li[Li_{0.2}Ni_{0.2}Mn_{0.6}]O_2$ electrode delivers discharge capacities of 200 and 240 mAh g^{-1} with excellent cycleability at 30 and 55 °C, respectively.

Keywords: Lithium secondary batteries; Sol–gel method; Layered manganese; Cathode materials; Li_2MnO_3

1. Introduction

Rechargeable lithium batteries have developed into a major technology during the past 10 years. The first commercial lithium-ion batteries, introduced in 1990, used $LiCoO_2$ for the positive electrode (cathode), and this material continues to be used in more than 90% of commercial lithium-ion batteries. Obviously, $LiCoO_2$ is an excellent cathode material with good capacity, reversibility and rate capability, but suffers from high cost and the relatively toxicity of cobalt. Research work in this area has focused attention mainly on $LiMn_2O_4$ and $LiMO_2$ (M = Ni, Mn) compounds [1–5]. These compounds crystallize in spinel-type and α-$NaFeO_2$ layered structures, respectively. $LiMn_2O_4$ has a smaller capacity than $LiCoO_2$, and is difficult to cycle in a rechargeable battery with the same stability. These disadvantages have not yet been overcome [6–9]. Lithium nickelate is also an attractive material for lithium-ion cells. Nevertheless, $LiNiO_2$ has some severe problems such as low discharge capacity (about 140–150 mAh g^{-1}) due to the difficult in the synthesis of stoichiometric $LiNiO_2$ and capacity decay due to the formation of the NiO_2 phase by the phase transition of the $LiNiO_2$ structure during intercalation–de-intercalation of lithium ions [10]. $LiMnO_2$ is a candidate as a positive electrode, but is hampered by the Jahn–Teller distortion exhibited by Mn^{3+} due mainly to the appearance of the spinel $LiMn_2O_4$ phase on cycling.

Recently, some research groups have attempted to stabilize the layered structure by using a solid solution between Li_2MnO_3 and $LiMO_2$ (M = Cr, Ni, Co) such as $Li[Li_{(1-2x)/3}Ni_xMn_{(2-x)/3}]O_2$ and $Li[Li_{(1-x)/3}Co(Cr)_xMn_{(2-2x)/3}]O_2$ [11–14]. Li_2MnO_3 ($Li[Li_{1/3}Mn_{2/3}]O_2$) has the same structure as $LiCoO_2$. Both $Li[Li_{x/3}Co_{1-x}Mn_{2x/3}]O_2$ and $Li[Li_{0.2}Cr_{0.4}Mn_{0.4}]O_2$ have Co^{3+} or Cr^{3+} partially replacing Li^+ and Mn^{4+} in $Li[Li_{1/3}Mn_{2/3}]O_2$, respectively, while maintaining the remaining Mn atoms in the 4+ oxidation state.

In this paper, a sol–gel method is employed to prepare layered $Li[Li_{(1-2x)/3}Ni_xMn_{(2-x)/3}]O_2$ powders using glycolic acid as a chelating agent. The structural and electrochemical properties of the materials are investigated and correlated to explain the electrochemical properties of the materials.

2. Experimental

$Li[Li_{(1-2x)/3}Ni_xMn_{(2-x)/3}]O_2$ ($x = 0.41$, 0.35, 0.275 and 0.2) powders were prepared by a sol–gel method using glycolic acid as a chelating agent. $Li(CH_3COO)\cdot 2H_2O$ (Kanto Chemical Co.), $Ni(CH_3COO)_2\cdot 4H_2O$ (Aldrich), and $Mn(CH_3COO)_2\cdot 4H_2O$ (Acros Organics) were dissolved in distilled water, and added dropwise to a continuously stirred aqueous solution of glycolic acid (Kanto Chemical Co.). The molar ratio of glycolic acid to total metal ions was unity. The pH of the solution was adjusted in the range 7–8

* Corresponding author. Tel.: +82-2-2290-0524; fax: +82-2-2282-7329.
E-mail address: yksun@hanyang.ac.kr (Y.-K. Sun).

0378-7753/02/$ – see front matter
PII: S0378-7753(02)00439-1

by adding ammonium hydroxide. The resultant solution was evaporated at 70–80 °C until a transparent sol was obtained. As the water evaporated further, the sol turned into a viscous transparent gel. The resulting gel precursors were decomposed at 480 °C for 5 h in air to eliminate the organic substances. The decomposed powders were pressed into pellets, heated at 900 °C for 3 h in air, and then quenched to room temperature.

Powder X-ray diffraction (Rigaku, Rint-2000) using Cu Kα radiation was used to identify the crystalline phase of the as-prepared powders. Rietveld refinement was then performed on the XRD data to obtain the lattice constants. Charge–discharge cycles were performed in CR2032 coin-type cells. The cell consisted of a cathode and a lithium metal anode separated by a porous polypropylene film. For fabrication of the electrode, the mixture, which contained 20 mg of $Li[Li_{(1-2x)/3}Ni_xMn_{(2-x)/3}]O_2$ powders and 12 mg conducting binder (8 mg of Teflonized acetylene black (TAB) and 4 mg of graphite), was pressed on 2.0 cm^2 stainless screen at 500 kg cm^{-2}. The electrolyte was a 1:2 mixture of ethylene carbonate (EC) and dimethyl carbonate (DMC) that contained 1 M $LiPF_6$ by volume. Charge–discharge cycling was performed galvanostatically at a current of 0.4 mA cm^{-2} (40 mA g^{-1}) at 30 and 55 °C in the voltage range 2.0–4.6 V and 2.4–4.5 V, respectively.

3. Results and discussion

The X-ray diffraction patterns of $Li[Li_{(L-2x)/3}Ni_xMn_{(2-x)/3}]O_2$ ($x = 0.41$, 0.35, 0.275 and 0.2) powders, with Millerindices indicated, are presented in Fig. 1. All the peaks can be indexed based on a hexagonal α-$NaFeO_2$ structure with space group *R3m*, which is characteristic of the layered $LiCoO_2$ and $LiNiO_2$ structures. The patterns show a single phase of a layered structure and are quite narrow. This indicates crystallinity of the materials. As can be seen in Fig. 1, a hexagonal phase (as indicated by splitting of (108) and (110) peaks) increases and diffraction peaks characteristic of Li_2MnO_3 (monoclinic phase) at $2\theta = 20$–25° increase with increasing Li concentration in $Li[Li_{(1-2x)/3}Ni_xMn_{(2-x)/3}]O_2$. The lattice parameters and *c*/*a* ratio are displayed as a function of *x* in $Li[Li_{(1-2x)/3}Ni_xMn_{(2-x)/3}]O_2$ in Fig. 2. While both *a* and *c* increase linearly with increasing nickel content, the *c*/*a* ratio decreases. This behavior indicates that Ni^{2+} ($r_{Ni^{2+}} = 0.69$ Å) is substituted for Li^+ ($r_{Li^+} = 0.76$ Å) and Mn^{4+} ($r_{Mn^{4+}} = 0.53$ Å) and a uniform solid solution is formed.

Typical voltage profiles of a Li|$Li[Li_{(1-2x)/3}Ni_xMn_{(2-x)/3}]O_2$ ($x = 0.41$, 0.35, 0.275 and 0.2) cell on the 10th cycle are shown in Fig. 3. The cells have smooth and monotonous charge–discharge curves and exhibit voltage profiles similar to those reported by other researchers [12–15]. There are significant irreversible capacity losses on the first cycle for the electrodes ($x = 0.41$, 0.35, 0.275 and 0.2), namely, 30–50 mAh g^{-1}.

The specific discharge capacities of Li|$Li[Li_{(1-2x)/3}Ni_xMn_{(2-x)/3}]O_2$ ($x = 0.2$, 0.275, 0.35, 0.41) cells as a function of cycle number at 30 °C is shown in Fig. 4. The cycling was carried out at a constant current density of 40 mA g^{-1} and between potential limits of 2.0 and 4.6 V. The discharge capacity of the $Li[Li_{0.06}Ni_{0.41}Mn_{0.53}]O_2$ electrode decreases with cycling. It is believed that the

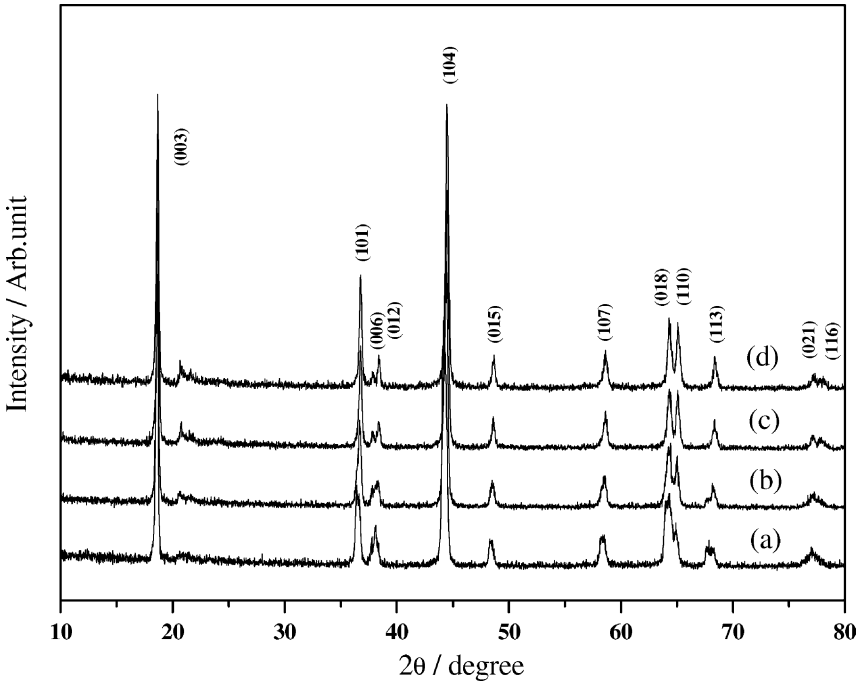

Fig. 1. X-ray diffraction patterns of $Li[Li_{(1-2x)/3}Ni_xMn_{(2-x)/3}]O_2$: (a) $x = 0.41$, (b) $x = 0.35$, (c) $x = 0.275$, (d) $x = 0.2$ powders.

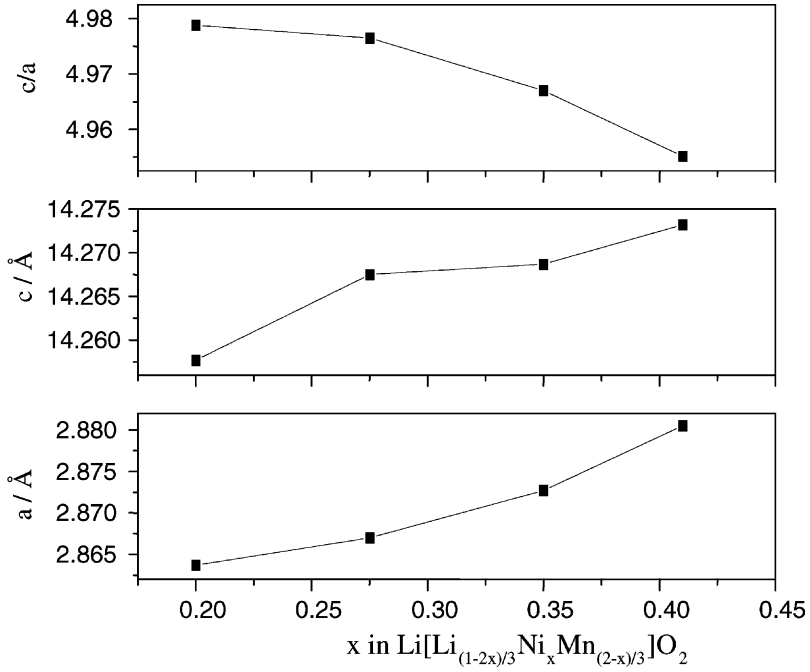

Fig. 2. Lattice constants and *c*/*a* ratio as function of x in $Li[Li_{(1-2x)/3}Ni_xMn_{(2-x)/3}]O_2$.

poor cycleability is attributed to the insufficiency of electrochemical inactive Li_2MnO_3 component, which contributes to stabilization of the $Li[Li_{(1-2x)/3}Ni_xMn_{(2-x)/3}]O_2$ host structure. It contains only Mn^{4+} and there are no crystallographic sites available for additional lithium intercalation [16]. The discharge capacities of the electrodes ($x = 0.35$, 0.275 and 0.2) increase slowly, and then stabilize within about 20th cycles. The discharge capacities of $Li[Li_{(1-2x)/3}Ni_xMn_{(2-x)/3}]O_2$ ($x = 0.41$, 0.35, 0.275 and 0.2) after 20th cycles deliver 156, 167, 188 and 200 mAh g^{-1}, respectively. All the electrodes, except for $x = 0.41$, show excellent cycleability.

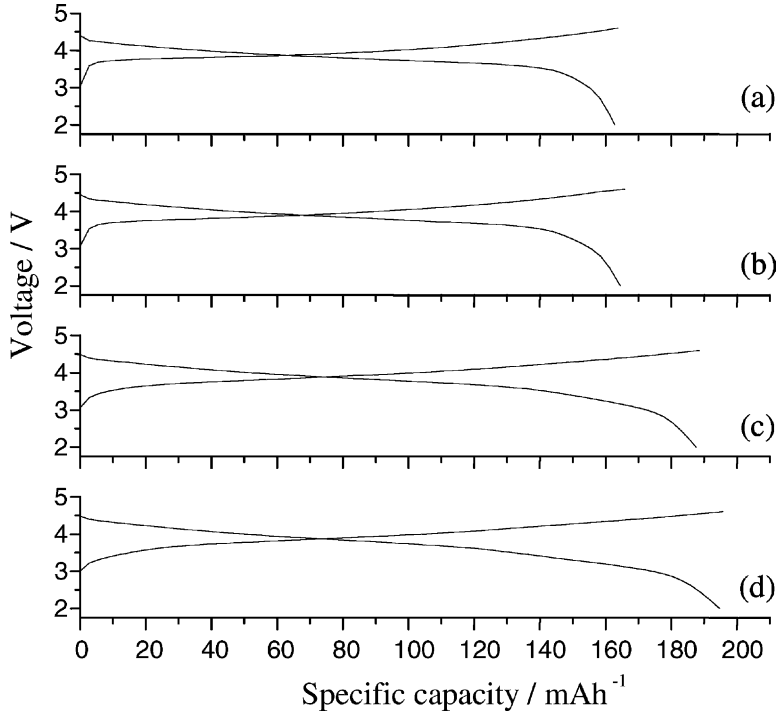

Fig. 3. The 10th charge–discharge curves of $Li|Li[Li_{(1-2x)/3}Ni_xMn_{(2-x)/3}]O_2$ cells; (a) $x = 0.41$, (b) $x = 0.35$, (c) $x = 0.275$, (d) $x = 0.2$ at rate of 0.4 mA cm^{-2} in voltages between 2.5 and 4.6 V.

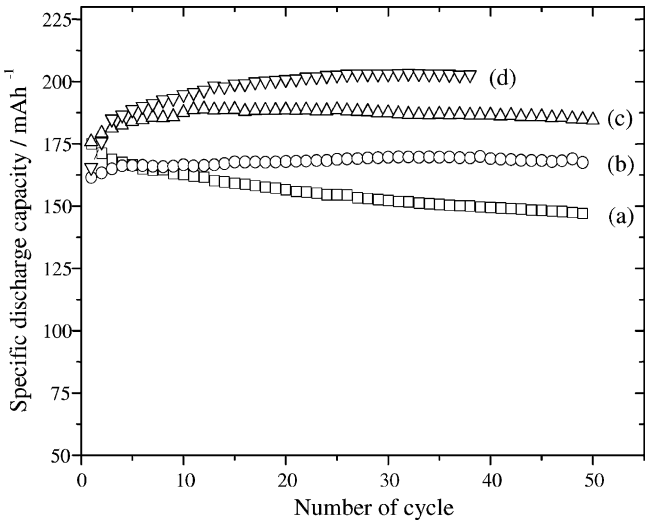

Fig. 4. Specific discharge capacity vs. cycle number of Li|Li[$Li_{(1-2x)/3}Ni_xMn_{(2-x)/3}$]$O_2$ cells at 30 °C; (a) $x = 0.41$, (b) $x = 0.35$, (c) $x = 0.275$, (d) $x = 0.2$.

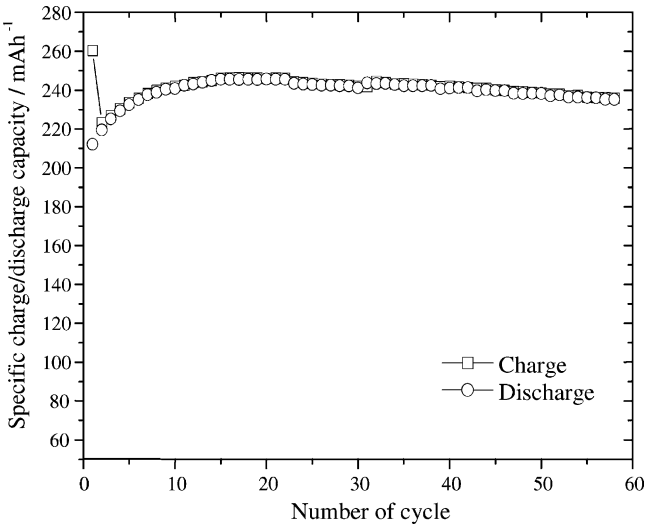

Fig. 5. Specific charge–discharge capacities vs. cycle number of Li|Li[$Li_{0.2}Ni_{0.2}Mn_{0.6}$]O_2 cells at high temperature (55 °C).

The charge/discharge capacity versus cycle number for the Li|Li[$Li_{0.2}Ni_{0.2}Mn_{0.6}$]O_2 cell at 55 °C in the voltage range 2.4–4.5 V is given in Fig. 5. The charge and discharge capacity of this electrode slowly increase during electrochemical cycling up to about 15 cycles, and subsequently stabilize on further cycling. The cell delivers a steady and high capacity of about 240 mAh g^{-1} and the charge–discharge efficiency is over 99% during the cycling.

Differential capacity versus voltage of plots Li[$Li_{0.1}Ni_{0.35}Mn_{0.55}$]$O_2$ and Li[$Li_{0.2}Ni_{0.2}Mn_{0.6}$]O_2 electrodes between 2.0 and 4.6 V at 30 °C are presented in Fig. 6. The important feature is the difference between the first and subsequent cycles. There is an oxidation peak near 4.6 V in the first oxidation process which is related to the irreversible capacity loss during the first charging. The data displayed in Fig. 6a and b are different from those for $LiNiO_2$, in that there are no three sharp peaks due to three distinct phase transitions. Major peaks for the charge and discharge process centered around 3.8 and 3.7 V, respectively, are shown in Fig. 6a. This result suggests that only one phase reaction should exist during the oxidation and reduction process, which indicates no expectation of structural degradation. Li[$Li_{0.2}Ni_{0.2}Mn_{0.6}$]O_2 shows a remarkable difference to the results in Fig. 6a, namely, the growth of peaks near 3.3 and 3.1 V with cycling during oxidation and reduction. It is considered that the growth of these peaks during the charge and discharge processes is the reason for the increase in capacity with increase in lithium concentration in Li[$Li_{(1-2x)/3}Ni_xMn_{(2-x)/3}$]$O_2$.

Given the theoretical capacities of the Li[$Li_{0.15}Ni_{0.275}Mn_{0.575}$]$O_2$ (167 mAh g^{-1}) and Li[$Li_{0.2}Ni_{0.2}Mn_{0.6}$]O_2 (126 mAh g^{-1}) electrodes based on Ni^{2+}/Ni^{4+} coupling, the delivered capacities of the materials are too large. Further studies are now in progress to reveal the unusual large capacity

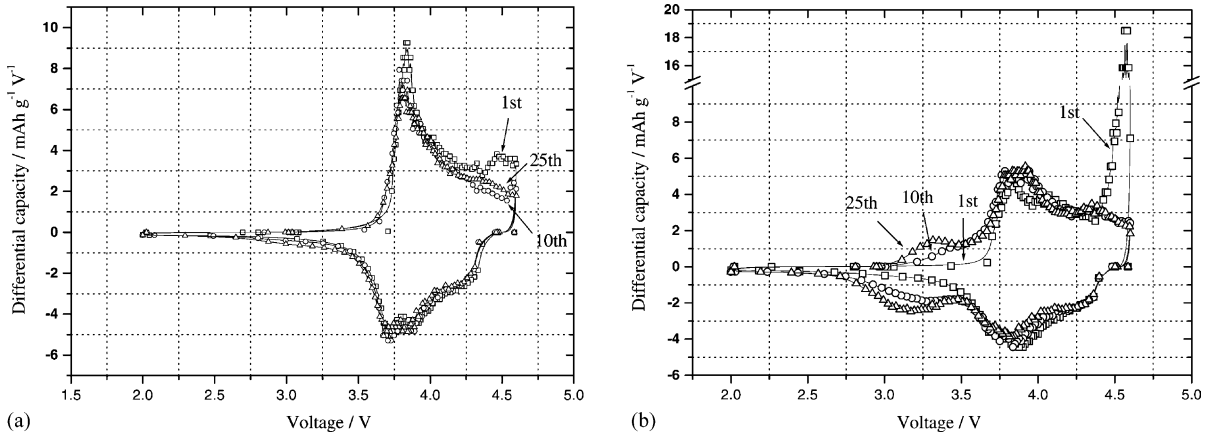

Fig. 6. Differential capacity vs. voltage of (a) Li[$Li_{0.1}Ni_{0.35}Mn_{0.55}$]$O_2$ and (b) Li[$Li_{0.2}Ni_{0.2}Mn_{0.6}$]O_2 electrodes between 2.0 and 4.6 V.

and structural stability of the $Li[Li_{(1-2x)/3}Ni_xMn_{(2-x)/3}]O_2$ materials.

4. Conclusions

Layered $Li[Li_{(1-2x)/3}Ni_xMn_{(2-x)/3}]O_2$ ($x = 0.41$, 0.35, 0.275 and 0.2) powders with high homogeneity and crystallinity have been synthesized by means of a sol–gel method. The layered structure solid solutions are obtained by Ni substitution for Li and Mn in Li_2MnO_3. The electrochemically inactive Li_2MnO_3 component contributes to stabilization of the $Li[Li_{(1-2x)/3}Ni_xMn_{(2-x)/3}]O_2$ host structure. The discharge capacity of the $Li[Li_{(1-2x)/3}Ni_xMn_{(2-x)/3}]O_2$ electrode increases with decrease Ni concentration. The $Li[Li_{0.2}Ni_{0.2}Mn_{0.6}]O_2$ electrode ($x = 0.2$) delivers a very high capacity of 200 and 240 mAh g^{-1} at 30 and 55 °C, respectively, with excellent cycleability.

Acknowledgements

This work is supported in part by the Ministry of Information & Communication of Korea (“Support Project of University Information Technology Research Center” supervised by KIPA).

References

[1] M.M. Thackeray, P.G. David, P.G. Bruce, J.B. Goodenough, Mat. Res. Bull. 18 (1983) 461.
[2] T. Ohzuka, M. Kitagawa, T. Hirai, J. Electrochem. Soc. 137 (1990) 769.
[3] D. Guyomard, J.-M. Tarascon, Solid State Ionics 69 (1994) 222.
[4] R.J. Gummow, A. de Kock, M.M. Thackeray, Solid State Ionics 69 (1994) 59.
[5] K. Amine, H. Tukamoto, H. Yasuda, Y. Fujita, J. Electrochem. Soc. 143 (1996) 1607.
[6] Y. Shao-Horn, S.A. Hackney, A.R. Armstrong, P.G. Bruce, R. Gitzendanner, C.S. Johnson, M.M. Thackeray, J. Eelectrochem. Soc. 146 (1999) 2404.
[7] A.R. Armstrong, R. Gitzendanner, A.D. Robertson, P.G. Bruce, Chem. Commun. (1988) 1833.
[8] Y.-I. Jang, B. Huang, Y.-M. Chiang, D.R. Sadoway, Electrochem. Solid State Lett. 1 (1998) 13.
[9] B. Ammundsen, J. Desilvestro, T. Groutso, D. Hassell, J.B. Metson, E. Regan, R. Steiner, P.J. Pickering, J. Eelectrochem. Soc. 147 (2000) 4078.
[10] T. Ohzuku, A. Ueda, M. Nagayama, J. Electrochem. Soc. 140 (1993) 1563.
[11] B. Ammundsen, J. Paulsen, Adv. Mat. 13 (2001) 943.
[12] K. Numata, C. Sakaki, S. Yamanaka, Solid State Ionics 117 (1999) 257.
[13] B. Ammundsen, J. Desilvestro, R. Steiner, P. Pickering, in: Proceedings of the 10th International Meeting on Lithium Batteries, vol. 97/98, Como, Italy, 28 May–2 June 2000.
[14] T. Ohzuku, Y. Makimura, Chem. Lett. (2001) 744.
[15] Z. Lu, D.D. MacNeil, J.R. Dahm, Electrochem. Solid State Lett. 4 (2001) A191.
[16] M.M. Thackeray, Prog. Solid State Chem. 25 (1997) 1.